ON INFORMATION ABOUT COVARIANCE PARAMETERS IN GAUSSIAN MATÉRN RANDOM FIELDS

Victor De Oliveira

Department of Management Science and Statistics

The University of Texas at San Antonio, U.S.A.

`victor.deoliveira@utsa.edu`

Zifei Han[1]

School of Statistics

University of International Business and Economics, China

`zifeihan@uibe.edu.cn`

Aug 29, 2022

(final version)

Abstract

The Matérn family of covariance functions is currently the most commonly used for the analysis of geostatistical data due to its ability to describe different smoothness behaviors. Yet, in many applications the smoothness parameter is set at an arbitrary value. This practice is due partly to computational challenges faced when attempting to estimate all covariance parameters and partly to unqualified claims in the literature stating that geostatistical data have little or no information about the smoothness parameter. This work critically investigates this claim and shows it is not true in general. Specifically, it is shown that the information the data have about the correlation parameters varies substantially depending on the true model and sampling design and, in particular, the information about the smoothness parameter can be large, in some cases larger than the information about the range parameter. In light of these findings, we suggest to reassess the aforementioned practice and instead establish inferences from data–based estimates of both range and smoothness parameters, especially for strongly dependent non–smooth processes observed on irregular sampling designs. A data set of daily rainfall totals is used to motivate the discussion and gauge this common practice.

Key words: Fisher information, Geostatistics, Microergodic parameter, Sampling design, Smoothness parameter.

---

[1]Corresponding author.

1   Introduction

Random fields are ubiquitous for the modeling of spatial and spatio–temporal data in most natural and earth sciences, such as ecology, epidemiology, geology and hydrology. Among these, Gaussian random fields play a prominent role due to their versatility to model spatially varying phenomena, and because they serve as building blocks for the construction of more sophisticated models (Zimmerman, 2010; Gelfand and Schliep, 2016). One of the common scientific goals in these sciences is spatial interpolation/prediction, and for this the covariance function of the random field plays a key role. Reliable modeling and inference of covariance functions of Gaussian random fields are then crucial steps toward this goal.

A large number of parametric families of covariance functions have appeared in the statistical literature, but just a few of them are commonly used in practice. One family that has reached prominence is the so–called *Matérn* family (Matérn, 1986). Except for a few sporadic appearances, this family was introduced in the statistical literature by Handcock and Stein (1993), and later Stein (1999) studied its properties and strongly advocated its use; see Guttorp and Gneiting (2006) for the history of this family. There are two main reasons that explain this prominence. First, unlike most other families that are indexed by a variance and a range parameter, covariance functions in the Matérn family also depend on an additional parameter, called the smoothness parameter, that controls the degree of mean square differentiability of the random field. Second, in a series of articles Stein (1988, 1990, 1993) established that, in the so–called fixed–domain asymptotic framework, it is possible to achieve efficient spatial interpolation with a misspecified covariance model, as long as the correct and misspecified models are compatible on the region of interest in some well defined sense. A necessary condition for two covariance functions from the Matérn family to be compatible in that sense is that they share the same smoothness parameter. The other parameters may differ, as long as these satisfy a certain relation (Zhang, 2004). This suggests that for efficient spatial interpolation/prediction using the Matérn family, correct specification of the smoothness parameter is critical and may even be more important than correct specification of the other parameters, at least in this particular asymptotic framework. The same situation has been recently found to hold for other families of covariance functions (Bevilacqua, Faouzi, Furrer, and Porcu, 2019).

In spite of the above, in some applied works there is a disconnect between theory and practice when it comes to modeling geostatistical data using the Matérn family. On the one hand, the facts stated above establish the importance of an adequate specification of the smoothness of the random field when the main goal is spatial prediction, which has been advocated by several researchers (Stein, 1999). On the other hand, the smoothness of the random field is oftentimes arbitrarily fixed in advance in these applied works rather than estimated. Even though there is usually little or no a priori information about the smoothness of the random field of interest, the exponential covariance family is commonly used as the

default model (a sub–family of the Matérn family) which is not mean square differentiable. This imposes from the onset a lack of smoothness in the random field, which may or may not be supported by the data. But gross misspecification of the smoothness of the random field likely precludes the possibility of efficient spatial interpolation/prediction. The same situation has been recently found to hold for other covariance families (Bevilacqua et al., 2019). This practice, somewhat common in geostatistics when estimating covariance functions, is motivated partly by numerical challenges practitioners sometimes face when attempting to estimate all parameters in the Matérn family, and partly by an unqualified claim in the literature stating that geostatistical data have little or no information about the smoothness of the random field. The latter has become part of the 'geostatistical folklore' in some applied quarters. The main aim of this work is to critically investigate this claim, and contribute to the bridging of theory and practice on this issue.

An area of application where this issue is especially relevant is the spatial modeling of rainfall fields. There are three (main) types of rainfall, depending on the atmospheric mechanism that triggers it: stratiform (predominant in northern–latitudes), convective (predominant in the tropics) and orographic (mountains). Rainfall from the former type tends to occur over large spatial scales, being of long duration, and varies slowly over space. On the other hand, rainfall from the latter two types tends to be more localized, being of short duration, with a very high gradient over short distances, with sharp transitions between the dry and wet sub–regions (Steiner, Houze, and Yuter, 1995). It is then expected that random fields that describe the spatial variation of stratiform rainfall to be smoother than random fields describing the spatial variation of convective and orographic rainfall. Consequently, rather than fixing the smoothness of the random field for rain data, a more satisfactory practice would be to estimate it, tailoring it to the type of atmospheric mechanism that generated the data.

Using the inverse diagonal elements of the inverse of the Fisher information matrix as a tool, this work investigates the information content that geostatistical data have about the covariance parameters of the Matérn family, with emphasis on the correlation parameters and a particular microergodic parameter. It is shown that the information about these parameters can vary widely depending on the true model and the sampling design, and the information about the smoothness parameter can be substantial, when the information about the range parameter is considered as reference. These findings cast doubt on the aforementioned claim, and invite to reassess the practice of fixing the smoothness parameter at an arbitrary value. A data set of daily rainfall totals collected in Switzerland is used to motivate the discussion and assess the aforementioned practice.

2   Data and Model

Geostatistical data consist of triplets $\{(\mathbf{s}_i, \boldsymbol{f}(\mathbf{s}_i), z_i) : i = 1, \ldots, n\}$, where $\mathcal{S}_n = \{\mathbf{s}_1, \ldots, \mathbf{s}_n\}$ is a set of sampling locations in the region of interest, called the *sampling design*, $\boldsymbol{f}(\mathbf{s}_i) = (f_1(\mathbf{s}_i), \ldots, f_p(\mathbf{s}_i))^\top$ is a p–dimensional vector of covariates measured at $\mathbf{s}_i$ (usually $f_1(\mathbf{s}) \equiv 1$), and z_i is a measurement of the quantity of interest collected at $\mathbf{s}_i$. The stochastic approach to spatial interpolation/prediction relies on viewing the set of measurements $\{z_i\}_{i=1}^n$ as a partial realization of a random field.

Let $\{Z(\mathbf{s}) : \mathbf{s} \in \mathcal{D}\}$ be a Gaussian random field with mean function $\mu(\mathbf{s})$ and covariance function $C(\mathbf{s}, \mathbf{u})$, with $\mathcal{D} \subset \mathbb{R}^d$ and $d \geq 1$. It would be assumed that $\mu(\mathbf{s}) = \sum_{j=1}^p \beta_j f_j(\mathbf{s})$, where $\boldsymbol{\beta} = (\beta_1, \ldots, \beta_p)^\top \in \mathbb{R}^p$ are unknown regression parameters. Additionally, $C(\mathbf{s}, \mathbf{u})$ is assumed isotropic and belonging to a parametric family, $\{C_{\boldsymbol{\theta}}(\mathbf{s}, \mathbf{u}) = \sigma^2 K_{\boldsymbol{\vartheta}}(||\mathbf{s} - \mathbf{u}||) : \boldsymbol{\theta} = (\sigma^2, \boldsymbol{\vartheta}) \in (0, \infty) \times \Theta\}$, $\Theta \subset \mathbb{R}^q$, where $K_{\boldsymbol{\vartheta}}(\cdot)$ is an isotropic correlation function in $\mathbb{R}^d$ and $||\cdot||$ is the Euclidean norm. Among the many possible isotropic covariance families, we focus in this work on the Matérn family with the parametrization proposed in Handcock and Stein (1993)

$$C_{\boldsymbol{\theta}}(r) = \frac{\sigma^2}{2^{\nu-1}\Gamma(\nu)} \left(\frac{2\sqrt{\nu}}{\vartheta} r \right)^\nu \mathcal{K}_\nu \left(\frac{2\sqrt{\nu}}{\vartheta} r \right), \qquad r \geq 0 \tag{2.1}$$
$$=: \sigma^2 K_{\boldsymbol{\vartheta}}(r),$$

where $r = ||\mathbf{s} - \mathbf{u}||$ is Euclidean distance between two locations, $\sigma^2 > 0$, $\boldsymbol{\vartheta} = (\vartheta, \nu) \in (0, \infty)^2$ are correlation parameters, $\Gamma(\cdot)$ is the gamma function and $\mathcal{K}_\nu(\cdot)$ is the modified Bessel function of second kind and order ν (Gradshteyn and Ryzhik, 2000, 8.40). For this family, $\sigma^2 = \mathrm{var}(Z(\mathbf{s}))$, ϑ (with units of distance) mostly controls how fast $C_{\boldsymbol{\theta}}(r)$ decays to zero when r increases, and ν (unitless) controls the degree of differentiability of $C_{\boldsymbol{\theta}}(r)$ at the origin. When $\nu > k$, $C_{\boldsymbol{\theta}}(\cdot)$ is $2k$ times differentiable at $r = 0$, which in turn implies that $Z(\cdot)$ is k–times mean square differentiable (Stein, 1999). Because of these properties, σ^2 is called the *variance* parameter, ϑ the *range* parameter and ν the *smoothness* parameter.

In applications the measurements z_i often contain measurement error, in which case they are modeled as

$$z_i = Z(\mathbf{s}_i) + \epsilon_i, \qquad i = 1, \ldots, n, \tag{2.2}$$

where $\epsilon_1, \ldots, \epsilon_n$ are i.i.d. with $\mathrm{N}(0, \tau^2)$ distribution and independent of $Z(\cdot)$; $\tau^2 \geq 0$ is called the *nugget* parameter. Although the findings in this work are likely to hold for other families of isotropic covariance functions, we focus on the Matérn family where the covariance structure of the data is indexed by $\boldsymbol{\eta} := (\sigma^2, \tau^2, \vartheta, \nu)$ and the smoothness parameter is considered unknown.

3 Smoothness Parameter: Fix or Estimate?

3.1 A Critical Look at a Geostatistical Practice

As indicated in the Introduction, the claim that geostatistical data have little or no information about the smoothness of the random field is sometimes seen in geostatistical practice (Bose, Hodges, and Banerjee, 2018, page 866). In addition, Diggle and Ribeiro (2007, page 113) state that "...when using the Matérn correlation function, our experience has been that the shape parameter κ [ν in (2.1)] is often poorly identified", and in page 114 they also state "...we have found that, for example, estimating all three parameters in the Matérn model is very difficult because the parameters are poorly identified, leading to ridges or plateaus in the log–likelihood surface." As a workaround these authors suggest using likelihood evaluations to select the smoothness parameter from a few candidate values, but this advice is often not followed. Statements like the ones above are sometimes interpreted in geostatistical practice as meaning that the data have little or no information about the smoothness parameter, prompting the practice of fixing the smoothness parameter at an arbitrary value. More often than not, the exponential model ($\nu = 1/2$) is used as the default model, and the other covariance parameters, variance, range and nugget are then estimated. But this interpretation is overly simplistic and not granted in general, since weak identifiability and an ill behavior of the likelihood surface both derive from the proposed model as a *whole*, and in general may not be attributable to a single parameter, especially when the parameters are highly non–orthogonal.

The practice of arbitrarily fixing the smoothness parameter assumes, perhaps implicitly, at least one of the two tenets: (a) the data contain more information about the variance and range parameters than about the smoothness parameter and/or (b) the variance and range parameters are more important for spatial interpolation/prediction than the smoothness parameter. However, there are theoretical and practical arguments that cast doubts about these tenets, at least for the Matérn family. It has been shown that, in the fixed–domain asymptotic framework, σ^2 and ϑ *cannot* be consistently estimated when $d \leq 3$ (Zhang, 2004). On the other hand, ν is what is called a *microergodic* parameter (Stein, 1999), so consistent estimation of ν is plausible. In fact, Wu, Lim, and Xiao (2013), Loh (2015), Wu and Lim (2016) and Loh, Sun, and Wen (2021) have constructed, under some conditions on the design and the true smoothness, estimators of ν that are consistent under fixed–domain asymptotics. Hence, the aforementioned practice is in conflict with these results, which indicate that geostatistical data may contain substantial information about the smoothness parameter, at least under the conditions for which the above results hold. Also, Kaufman and Shaby (2013, Theorem 3) have shown that for any prediction location $\mathbf{s}_0$, the best linear predictor of $Z(\mathbf{s}_0)$ based on a misspecified Matérn model is (fixed–domain) asymptotically efficient when ν is correctly specified, regardless of the values of σ^2 and ϑ.
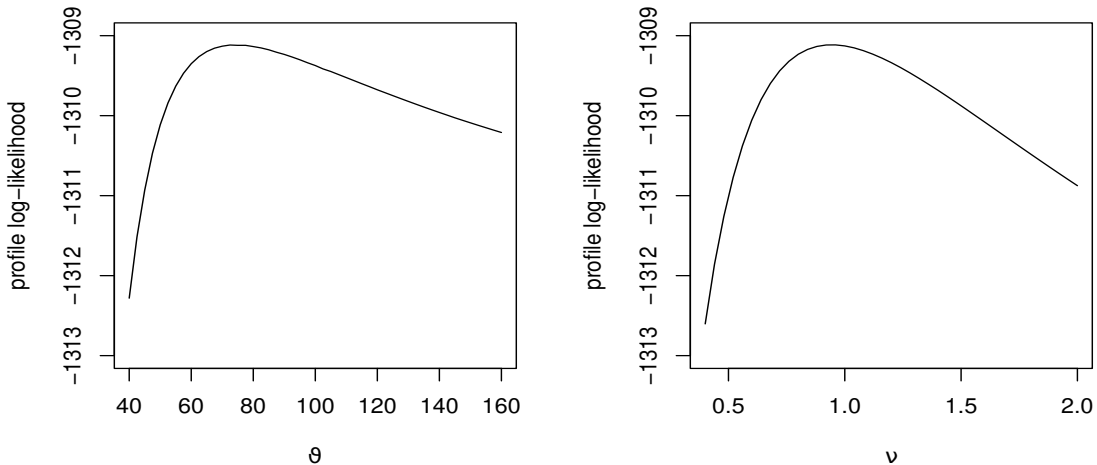
Figure 1: Profile log–likelihood of ϑ (left) and ν (right) for the Swiss rainfall data.

The next section provides a practical example that casts doubt on the implicit two tenets mentioned above.

In this work we show that these tenets do not always hold, and investigate a more satisfactory practice to quantify information about covariance parameters based on the study of likelihood functions. It is shown that the actual situation is much more nuanced than the above claim suggests, and that the information the data contain about the smoothness parameter depends critically on aspects of the true model and observed data, in particular on the sampling design $\mathcal{S}_n$.

3.2   A Telling Example

In this section the rainfall data set analyzed in Diggle and Ribeiro (2007, Section 5.4.7) is used to show that the claim of spatial data not being informative about the smoothness parameter does not hold. This data set is available from the R package geoR. The data consists of 467 measurements of daily rainfall collected in Switzerland on May 8, 1986, using an irregular sampling design where the coordinates of the sampling locations were measured in kilometers. The model for the (square root transformed) data is of the form (2.2), where $Z(\cdot)$ is a Gaussian random field with constant mean and the Matérn covariance function (2.1). The maximum likelihood estimates of the covariance parameters are $\hat{\boldsymbol{\eta}} = (\hat{\sigma}^2, \hat{\tau}^2, \hat{\vartheta}, \hat{\nu}) = (105.09, 6.74, 73.42, 0.95)$. The information about the covariance parameters $\boldsymbol{\eta}$ may be quantified by inspecting the observed information matrix, $H(\hat{\boldsymbol{\eta}})$. An approximation to this matrix is usually provided by the optimization algorithm, denoted as

$\hat{H}$. For the Swiss rainfall data, the inverse of this matrix is given by

$$\hat{H}^{-1} = \begin{pmatrix} 1720.183 & -5.633 & 838.860 & -2.431 \\ -5.633 & 2.817 & -17.850 & 0.474 \\ 838.860 & -17.850 & 626.629 & -5.223 \\ -2.431 & 0.474 & -5.223 & 0.105 \end{pmatrix}. \tag{3.1}$$

For multiparameter cases, the information about a parameter may be measured by the inverse of the Cramer–Rao lower bound for the variance of unbiased estimators of that parameter. For ν say, this is estimated by $1/\hat{H}^{\nu\nu}$, with $\hat{H}^{\nu\nu}$ denoting the '(ν, ν)' diagonal element of $\hat{H}^{-1}$. For the Swiss rainfall data $1/\hat{H}^{\nu\nu} = 9.524$, suggesting that these data contain substantial information about ν. Also, $1/\hat{H}^{\vartheta\vartheta} = 0.0016$. Although this might suggest that these data are more informative about ν than about ϑ, this is not necessarily the case since the information about ϑ depends on the (arbitrary) units used to measure distance (e.g., kilometers versus meters). In Section 4.3 a re–scaling of the spatial coordinates is used so that the information about the range and smoothness parameters can be more sensibly compared, and this is used in Section 5.1 to re–analyze this data set. An equivalent visual approach to quantify information about the individual parameters is to inspect their profile log–likelihoods, $\text{pl}_1(\vartheta)$ and $\text{pl}_2(\nu)$ displayed in Figure 1. Although the degree of "peakness" appears similar in both graphs, the curvatures of these graphs at their maxima are quite different, $-(\partial^2/\partial\vartheta^2)\text{pl}_1(\vartheta)\big|_{\vartheta=\hat{\vartheta}} \approx 1/\hat{H}^{\vartheta\vartheta} = 0.0016$ and $-(\partial^2/\partial\nu^2)\text{pl}_2(\nu)\big|_{\nu=\hat{\nu}} \approx 1/\hat{H}^{\nu\nu} = 9.524$ (Seber and Wild, 2003) (the approximation is due to the use of the approximate rather than exact observed information matrix). Zhu and Zhang (2006) provided another example of a data set that appears to contain substantial information about the smoothness parameter. The likelihood summaries reported in this section were obtained using the R package georob (Papritz and Schwierz, 2021).

Since ϑ and ν are non–orthogonal and they are not the only model parameters, a more complete analysis also involves the inspection of joint profile log–likelihoods for all pairs of covariance parameters. For the Swiss rainfall data, the contour plots of the joint profile log–likelihoods of (ϑ, ν), (σ^2, ν), (σ^2, ϑ), (τ^2, ν), (τ^2, ϑ) and (σ^2, τ^2) are displayed in Figure 2. The joint profile log–likelihood of (ϑ, ν) displays a plateau, showing that the MLEs of these parameters are highly interdependent. A similar but more extreme behavior is displayed by the joint profile log–likelihoods of (σ^2, ϑ) and (τ^2, ν). On the other hand, the joint profile log–likelihood of (σ^2, ν) does not display a plateau as its curvature at the maximum is much larger than that of the others, and a similar behavior holds for the joint profile likelihood of (σ^2, τ^2). Together these plots suggest that the data might be more informative about (σ^2, ν) than about the other covariance parameters.
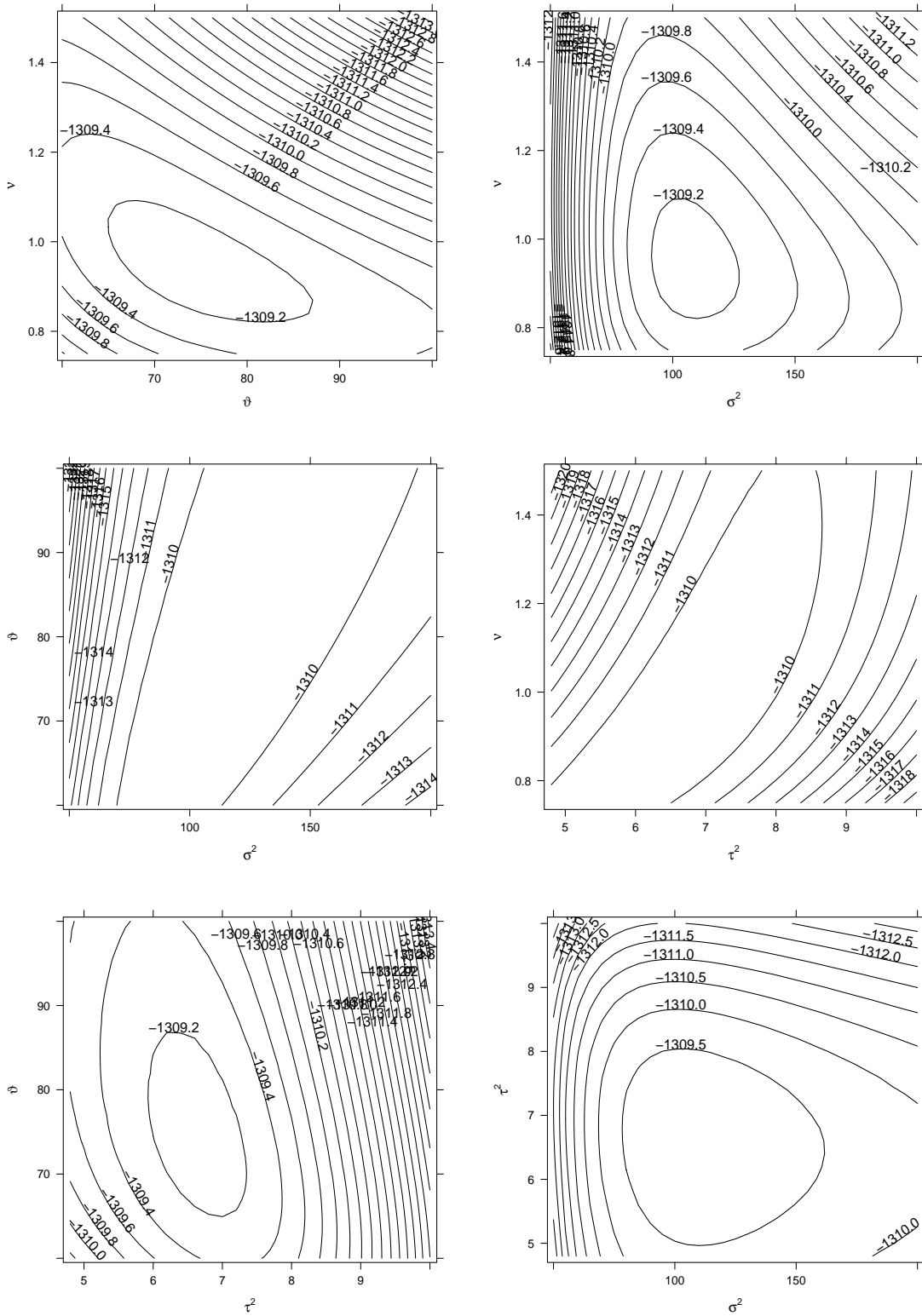
Figure 2: Joint profile log–likelihoods of all pairs of parameters in $\boldsymbol{\eta}$ for the Swiss rainfall data.

3.3 Interplay Between Smoothness and Nugget

It has been empirically observed by several authors and us, using both simulated and real data sets, that the estimate of the nugget parameter is closely related to the assumed smoothness of the random field. Specifically, the more smooth the random field is assumed, the larger the estimate of the nugget; see Diggle and Ribeiro (2007, Tables 5.1 and 5.2) and Figure 2 (middle right panel). This is intuitively expected: 'discordant' observations collected at close by locations might be explained either as coming from a non–smooth random field model or due to the presence of measurement error. If the smoothness were to be fixed at a value that is higher than the one supported by the data, an overestimation of the nugget would result to compensate. The opposite effect is expected when the smoothness is fixed at a value that is too low. As an illustration, if when fitting the Swiss rainfall data the smoothness parameter is fixed in advance at the values $\nu = 0.5$, 1 and 1.5, the corresponding estimates of the nugget are $\hat{\tau}^2 = 2.48$, 6.90 and 8.17, respectively.

From the above follows that arbitrarily fixing the smoothness parameter may result in a substantial misspecification of the nugget parameter, which has consequences for spatial prediction. When the data contain measurement error, the so–called nugget–to–sill ratio, $\tau^2/(\sigma^2+\tau^2)$, controls the amount of 'smoothing' (as opposed to interpolation) that is carried out on the data for spatial prediction. For the Swiss rainfall data, the estimated nugget–to–sill ratios are 0.02, 0.06 and 0.08 when the smoothness parameter is fixed at one of the aforementioned values. Estimating the smoothness parameter from the data, rather than fixing it, may avoid an undue dependence of the estimated nugget (and nugget–to–sill ratio) on a possibly grossly misspecified smoothness.

4 Quantifying Information About Covariance Parameters

In this section we carry out a numerical exploration to uncover the extent to which the sampling design and true model affect the information content the data have about co-variance parameters. We consider several sampling designs in the plane ($d = 2$) that are commonly used in geostatistical practice, and describe a new way to efficiently compute the Fisher information matrix for the Matérn model. As in the example in Section 3.2, the information content about each covariance parameter is measured by the vector

$$\text{Inf}(\boldsymbol{\eta}, \mathcal{S}_n) := \left(\frac{1}{I(\boldsymbol{\eta}, \mathcal{S}_n)^{\sigma^2\sigma^2}}, \frac{1}{I(\boldsymbol{\eta}, \mathcal{S}_n)^{\tau^2\tau^2}}, \frac{1}{I(\boldsymbol{\eta}, \mathcal{S}_n)^{\vartheta\vartheta}}, \frac{1}{I(\boldsymbol{\eta}, \mathcal{S}_n)^{\nu\nu}} \right), \qquad (4.1)$$

where $I(\boldsymbol{\eta}, \mathcal{S}_n)^{\sigma^2\sigma^2}$, $I(\boldsymbol{\eta}, \mathcal{S}_n)^{\tau^2\tau^2}$, $I(\boldsymbol{\eta}, \mathcal{S}_n)^{\vartheta\vartheta}$ and $I(\boldsymbol{\eta}, \mathcal{S}_n)^{\nu\nu}$ are, respectively, the first, second, third and fourth diagonal elements of $I(\boldsymbol{\eta}, \mathcal{S}_n)^{-1}$, and $I(\boldsymbol{\eta}, \mathcal{S}_n)$ is the Fisher information matrix based on the sampling design $\mathcal{S}_n$ when the true covariance parameter is $\boldsymbol{\eta}$.

4.1 Sampling Designs

It is well established in the geostatistical literature that the sampling design exerts a substantial effect on the properties of parameter estimators and predictors. Designs that are most favorable for parameter estimation are quite different from those that are most favorable for spatial prediction, under the assumption that the parameters are known (Zhu and Stein, 2005; Zhu and Zhang, 2006; Zimmerman, 2006). Designs that are optimal for covariance function estimation are irregular, in the sense that they include a substantial fraction of clustered or closely spaced sampling locations, while designs that are optimal for spatial prediction tend to be regular or 'space filling'. Because of this, some 'hybrid' designs have been proposed that supplement a set of regularly spaced sampling locations with a set of closely spaced sampling locations, with the intent of balancing the (conflicting) requirements for adequate covariance estimation and spatial prediction. See Diggle and Lophaven (2006), Zhu and Stein (2006) and Zimmerman (2006) for examples of hybrid designs.

To assess the effect of the sampling design $\mathcal{S}_n$ on the amount of information the data have about covariance parameters, we consider the four types of sampling designs described below, which are commonly used in practice. For concreteness, in the exploration in Section 4.3 we define these sampling designs for the region $\mathcal{D} = [0, 1] \times [0, 1]$ and sample size $n = 225$ or 226, but they can be equally defined for other regions and sample sizes.

Regular. This is a deterministic design where the sampling locations form a 15×15 regular lattice in $\mathcal{D}$; the distance between neighboring sampling locations is $r_{\min} = 1/15 \approx 0.066$. This design is preferred when the goal is spatial prediction with a known model.

Random. This is a random design where the sampling locations are a random sample of size 225 from the $\text{unif}\big((0, 1)^2\big)$ distribution. This design is preferred when the goal is to estimate the covariance parameters.

Bachoc. This is a class of random designs proposed by Bachoc (2014) and is constructed as follows. For $n = n_1 n_2$, with $n_1, n_2 \in \mathbb{N}$, let $\mathbf{v}_1, \ldots, \mathbf{v}_n$ be a set of points in $\mathcal{D}$ that form a regular lattice with distance $\Delta > 0$ between neighboring $\mathbf{v}_i$s, and $\mathbf{X}_1, \ldots, \mathbf{X}_n$ be a set of i.i.d. random vectors with a distribution symmetric about $\mathbf{0}_2$ and with support contained in $(-\Delta, \Delta)^2$. The sampling design $\mathcal{S}_n$ is assumed to be a realization of the set $\{\mathbf{v}_1 + \epsilon \mathbf{X}_1, \ldots, \mathbf{v}_n + \epsilon \mathbf{X}_n\}$ for some $\epsilon \in [0, 1/2)$. By varying the tuning constant ϵ this scheme can generate a continuum of designs that range from regular ($\epsilon = 0$) to moderately irregular ($\epsilon \approx 1/2$). We assume in Section 4.3 that $n_1 = n_2 = 15$, $\Delta = 1/15$, $\epsilon = 0.4$ and $\mathbf{X}_i \sim \text{unif}\big((-\Delta, \Delta)^2\big)$.

Regular+Cluster. This is a class of random designs consisting of a set of points in a regular design supplemented with several sets of highly clustered points. It is constructed in two steps as follows. First, $n_1 \times n_1$ sampling locations are selected that form a regular lattice in $\mathcal{D}$. Second, nc points are selected at random (without replacement) from the n_1^2
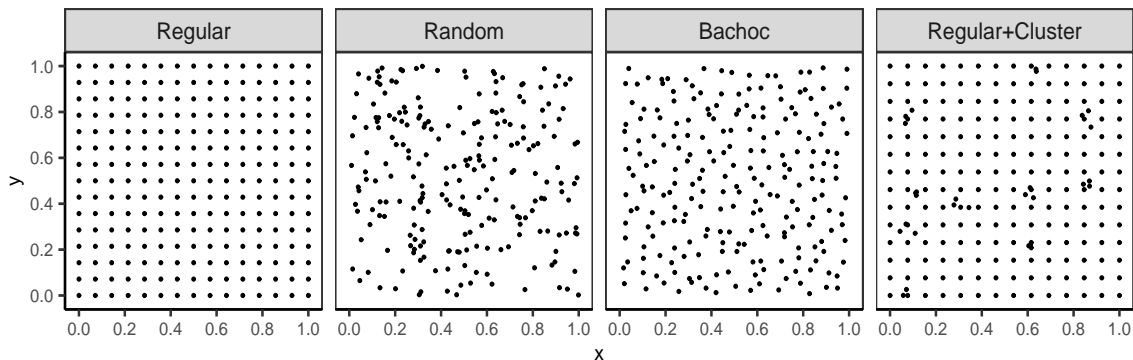
Figure 3: Examples of four different sampling design types in $\mathcal{D} = [0,1] \times [0,1]$.

points in the first step to serve as cluster centers. Then for each cluster center, $\mathbf{v}_i$ say, a set of $ppc - 1$ points is generated independently and uniformly distributed around the cluster center as $\mathbf{v}_i + \mathbf{w}_{ij}$, with $\mathbf{w}_{ij} \sim \text{unif}((-\epsilon, \epsilon)^2)$ for some $\epsilon > 0$. This is a kind of 'hybrid' design with $n = n_1^2 + nc(ppc - 1)$ sampling locations that seeks to balance the requirements for adequate covariance estimation and spatial prediction. We assume in Section 4.3 that $n_1 = 14$, $nc = 10$, $ppc = 4$ and $\epsilon = 0.04$.

The above sampling designs are illustrated in Figure 3, where a generic sampling location $\mathbf{s}$ in a design has Cartesian coordinates (x, y).

4.2 Computation of Fisher Information Matrix: Matérn Model

The results reported in Section 3.2 used an approximation of the *observed* information matrix based on difference quotients, as provided by the output of the optimization algorithm. But this can be a poor approximation to the *Fisher* information matrix. A more reliable alternative would be to use an explicit expression for the Fisher information matrix, when this is available. Let $\boldsymbol{\eta} = (\eta_1, \eta_2, \eta_3, \eta_4) = (\sigma^2, \tau^2, \vartheta, \nu)$ be the covariance parameters. For Gaussian random fields the Fisher information matrix of $\boldsymbol{\eta}$ based on the data model in (2.2) is the 4×4 matrix $I(\boldsymbol{\eta}, \mathcal{S}_n)$ with entries (Cressie, 1993; Stein, 1999)

$$I(\boldsymbol{\eta}, \mathcal{S}_n)_{ij} = \frac{1}{2}\text{tr}\big(\Psi^{-1}(\boldsymbol{\eta}, \mathcal{S}_n)\Psi_i(\boldsymbol{\eta}, \mathcal{S}_n)\Psi^{-1}(\boldsymbol{\eta}, \mathcal{S}_n)\Psi_j(\boldsymbol{\eta}, \mathcal{S}_n)\big), \qquad (4.2)$$

where $\Psi(\boldsymbol{\eta}, \mathcal{S}_n) := \sigma^2\boldsymbol{\Sigma_{\vartheta}} + \tau^2\boldsymbol{I}_n$, $\boldsymbol{\Sigma_{\vartheta}}$ is the $n \times n$ matrix with entries $(\boldsymbol{\Sigma_{\vartheta}})_{ij} = K_{\boldsymbol{\vartheta}}(\|\mathbf{s}_i - \mathbf{s}_j\|)$, $\boldsymbol{\vartheta} = (\vartheta, \nu)$, $\boldsymbol{I}_n$ is the $n \times n$ identity matrix and $\Psi_i(\boldsymbol{\eta}, \mathcal{S}_n) := \frac{\partial}{\partial \eta_i}\Psi(\boldsymbol{\eta}, \mathcal{S}_n)$, where these derivatives are computed entry–wise. The above matrices do not depend on p nor the regression parameters $\boldsymbol{\beta}$. For the Matérn model, the computation of some of the entries of $I(\boldsymbol{\eta}, \mathcal{S}_n)$ requires computing derivatives of the Bessel function $\mathcal{K}_\nu(x)$, both with respect to x and ν. For the former derivative it holds that (Gradshteyn and Ryzhik, 2000, 8.486–12)

$$\frac{\partial}{\partial x}\mathcal{K}_\nu(x) = -\Big(\mathcal{K}_{\nu-1}(x) + \frac{\nu}{x}\mathcal{K}_\nu(x)\Big), \qquad x \neq 0, \qquad (4.3)$$

so this can be computed exactly from the code that computes this Bessel function (e.g., the R function `besselK`). For the latter derivative and when $\nu = m$ is a non–negative integer, it holds that (Gradshteyn and Ryzhik, 2000, 8.486(1)–9)

$$\frac{\partial}{\partial \nu} \mathcal{K}_\nu(x) \Big|_{\nu=m} = \frac{m!}{2} \sum_{j=0}^{m-1} \frac{(x/2)^{j-m} \mathcal{K}_j(x)}{j!(m-j)}, \tag{4.4}$$

so again this can be computed from the code that computes this Bessel function. On the other hand, it seems to be few algorithms available to compute this derivative when ν is not a non–negative integer. An approach to compute this derivative for an arbitrary value of ν is to use a representation of this Bessel function that is amenable to exact differentiation. One such representation is given by (Gradshteyn and Ryzhik, 2000, 8.432–1)

$$\mathcal{K}_\nu(x) = \int_0^\infty e^{-x \cosh(t)} \cosh(\nu t) dt,$$

from which it follows that

$$\frac{\partial}{\partial \nu} \mathcal{K}_\nu(x) = \int_0^\infty t e^{-x \cosh(t)} \sinh(\nu t) dt. \tag{4.5}$$

Using (4.3) and (4.5) we have that for any $\boldsymbol{\vartheta} \in (0, \infty)^2$ and $r \geq 0$

$$\frac{\partial}{\partial \vartheta} K_{\boldsymbol{\vartheta}}(r) = \frac{4\nu^{\frac{\nu+1}{2}} r^{\nu+1}}{\Gamma(\nu) \vartheta^{\nu+2}} \mathcal{K}_{\nu-1}\left(\frac{2\sqrt{\nu}}{\vartheta} r\right), \tag{4.6}$$

where $K_{\boldsymbol{\vartheta}}(r)$ is the Matérn correlation function defined in (2.1) and

$$\frac{\partial}{\partial \nu} K_{\boldsymbol{\vartheta}}(r) = \left(\log\left(\frac{\sqrt{\nu}}{\vartheta} r\right) - \psi(\nu)\right) K_{\boldsymbol{\vartheta}}(r) \tag{4.7}$$

$$- h(\nu)\left(\frac{r}{\vartheta\sqrt{\nu}} \mathcal{K}_{\nu-1}\left(\frac{2\sqrt{\nu}}{\vartheta} r\right) - \int_0^\infty t \sinh(\nu t) \exp\left(-\frac{2r\sqrt{\nu}}{\vartheta} \cosh(t)\right) dt\right),$$

where $\psi(\nu)$ is the digamma function and

$$h(\nu) := \frac{2}{\Gamma(\nu)}\left(\frac{\sqrt{\nu}}{\vartheta} r\right)^\nu;$$

the derivations of the above identities are given in the Appendix. For any $\nu > 0$ and $w := 2r\sqrt{\nu}/\vartheta > 0$, inspection of the integrand of the integral in (4.7) reveals that it is a positive, smooth and unimodal function that converges to zero very fast as t approaches zero or infinity. Approximation of this integral (e.g., using the R function `integrate`) is relatively fast and accurate for the purpose at hand (but see Section 6). For instance, for a variety of test combinations of $w > 0$ and $\nu = m$ a non–negative integer, it was found that these approximations to $(\partial/\partial\nu)K_{\boldsymbol{\vartheta}}(r)$ are indistinguishable from the exact values obtained by using (4.4).

4.3 Numerical Exploration of Information Patterns

In this subsection we explore the patterns of variation of the information defined in (4.1) under various model settings and sampling designs. Consider collecting data in the region of the plane $\mathcal{D} = [0,1] \times [0,1]$ that follow model (2.2) with $C_{\boldsymbol{\theta}}(r)$ the Matérn covariance function in (2.1). Without loss of generality we assume $p = 1$ and $\beta = 0$. For the sampling designs $\mathcal{S}_n$ defined in Section 4.1 and a set of representative covariance parameters $\boldsymbol{\eta}$, we explore the variation of the last two components of the information vector $\mathrm{Inf}(\boldsymbol{\eta}, \mathcal{S}_n)$ in (4.1) as well as that of a particular microergodic parameter; a similar but more limited exploration was reported in (Stein, 1999, Section 6.6) for processes in the line. For the rest of this section the spatial coordinates are re–scaled. Specifically, we use new coordinates defined as $\tilde{\mathbf{s}} = (\tilde{x}, \tilde{y}) := \mathbf{s}/r_{\max}$, where $r_{\max} := \max\{\|\mathbf{s} - \mathbf{u}\| : \mathbf{s}, \mathbf{u} \in \mathcal{D}\}$; $\tilde{\mathbf{s}} := (x, y)/\sqrt{2}$ for the aforementioned region $\mathcal{D}$. Then, the re–scaled coordinates are unitless and invariant to the units of the original coordinates, and consequently so is the range parameter. The purpose of the re–scaling is to be able to compare more sensibly the information about the range and smoothness parameters, so the former may serve as a reference to judge when the latter is substantial. Although other re–scalings are possible, all produce the same effect, namely, making the range parameter unitless while changing little the information about the other covariance parameters.

Except for the regular design, the other three designs are random, and so is $\mathrm{Inf}(\boldsymbol{\eta}, \mathcal{S}_n)$. Nevertheless, numerical inspection of $\mathrm{Inf}(\boldsymbol{\eta}, \mathcal{S}_n)$ reveals that, when the covariance parameters are kept fixed, the entries of this vector vary very little over different realizations of the same design type (of the same size), and the same holds for their ordering. Because of this, we ignore the stochastic nature of $\mathrm{Inf}(\boldsymbol{\eta}, \mathcal{S}_n)$ and investigate the patterns of variation for a single realization of each of the considered sampling designs. As for the covariance parameters, we fix $\sigma^2 = 1$ and $\tau^2 = 0.2$ and explore the variations of the last two components of $\mathrm{Inf}(\boldsymbol{\eta}, \mathcal{S}_n)$, denoted $\mathrm{Inf}(\boldsymbol{\eta}, \mathcal{S}_n)_3$ and $\mathrm{Inf}(\boldsymbol{\eta}, \mathcal{S}_n)_4$, as a function of the correlation parameters in a grid of points (ϑ, ν) in $[0.05, 0.65] \times [0.1, 1.5]$. This set of correlation parameters includes range parameters that are practically relevant for the region $\mathcal{D}$ and smoothness parameters that are commonly found in geostatistical practice.

Information About the Range Parameter. We first investigate the variation of the information about the range parameter ϑ, both as a function of ϑ and as a function of ν.

Figure 4 (top panels) displays plots of $\mathrm{Inf}(\boldsymbol{\eta}, \mathcal{S}_n)_3$ as a function of ϑ when $\nu = 0.5$ and 1.5 for the four sampling designs. For both values of the smoothness parameter and all the designs but the Regular, the information about ϑ decreases monotonically when ϑ increases, which is expected as the 'effective sample size' decreases when the strength of spatial correlation increases. The Regular design departs slightly from this pattern for small values of ϑ. Also, regardless of the design and the range parameter, the information about ϑ is larger when $\nu = 1.5$ than when $\nu = 0.5$. A possible explanation for this pattern (and a

13

similar one described in the paragraph below) is that realizations of smooth processes are less oscillatory than those of non–smooth processes, so the strength of correlation can be better assessed based on data from the former. In addition, the information about ϑ is very small when the spatial correlation is strong and, for most models, the information about the range parameter is quite similar across all the designs.

Figure 4 (bottom panels) displays plots of $\mathrm{Inf}(\boldsymbol{\eta}, \mathcal{S}_n)_3$ as a function of ν when $\vartheta = 0.2$ and 0.5 for the four sampling designs. For both values of the range parameter and all the designs, the information about ϑ increases monotonically when ν increases. The rate of increase is fast when $\vartheta = 0.2$ while it is very slow when $\vartheta = 0.5$. Also, regardless of the design and the smoothness parameter, the information about ϑ is substantially larger when $\vartheta = 0.2$ than when $\vartheta = 0.5$. In addition, the information about ϑ is very large when the spatial correlation is weak and the process is smooth, and once again the information about the range parameter displays little sensitivity to the different designs. Overall, the plots in Figure 4 support the common empirical finding that inference about range parameters is difficult when the data are highly correlated, but they also suggest that this challenge abates somewhat for smooth processes.

Information About the Smoothness Parameter. Next we investigate the variation of the information about the smoothness parameter ν, both as a function of ϑ and as a function of ν.

Figure 5 (top panels) displays plots of $\mathrm{Inf}(\boldsymbol{\eta}, \mathcal{S}_n)_4$ as a function of ϑ when $\nu = 0.5$ and 1.5 for the four sampling designs. For both values of the smoothness parameter and all the designs, the information about ν appears to increase monotonically when ϑ increases, and this information is larger when $\nu = 0.5$ than when $\nu = 1.5$. When $\nu = 0.5$ the rate of increase in information is fast for small values of ϑ, but slow for large values, to the point that the information becomes close to constant, especially for the Random and Regular+Cluster designs. When $\nu = 1.5$ the information about ν is about constant and is small for all range parameters. Everything else being equal, the Regular design is the least informative about ν while the Random design is the most informative. The presence of many nearby pairs of sampling locations in the latter design enables better inference of smoothness.

Figure 5 (bottom panels) displays plots of $\mathrm{Inf}(\boldsymbol{\eta}, \mathcal{S}_n)_4$ as a function of ν when $\vartheta = 0.15$ and 0.35 for the four sampling designs. For both values of the range parameter and all designs, the information about ν generally increases up to a point and then decreases monotonically. Curiously, for all designs the information about ν peaks around the same value of ν (≈ 0.25). In addition, regardless of the design and the smoothness parameter, the information about ν is larger when $\vartheta = 0.35$ than when $\vartheta = 0.15$. Overall, this information becomes very small when the process is smooth, but for non–smooth processes the information depends substantially on the design. Again, the Regular design is the least informative about ν while the Random design is the most informative.
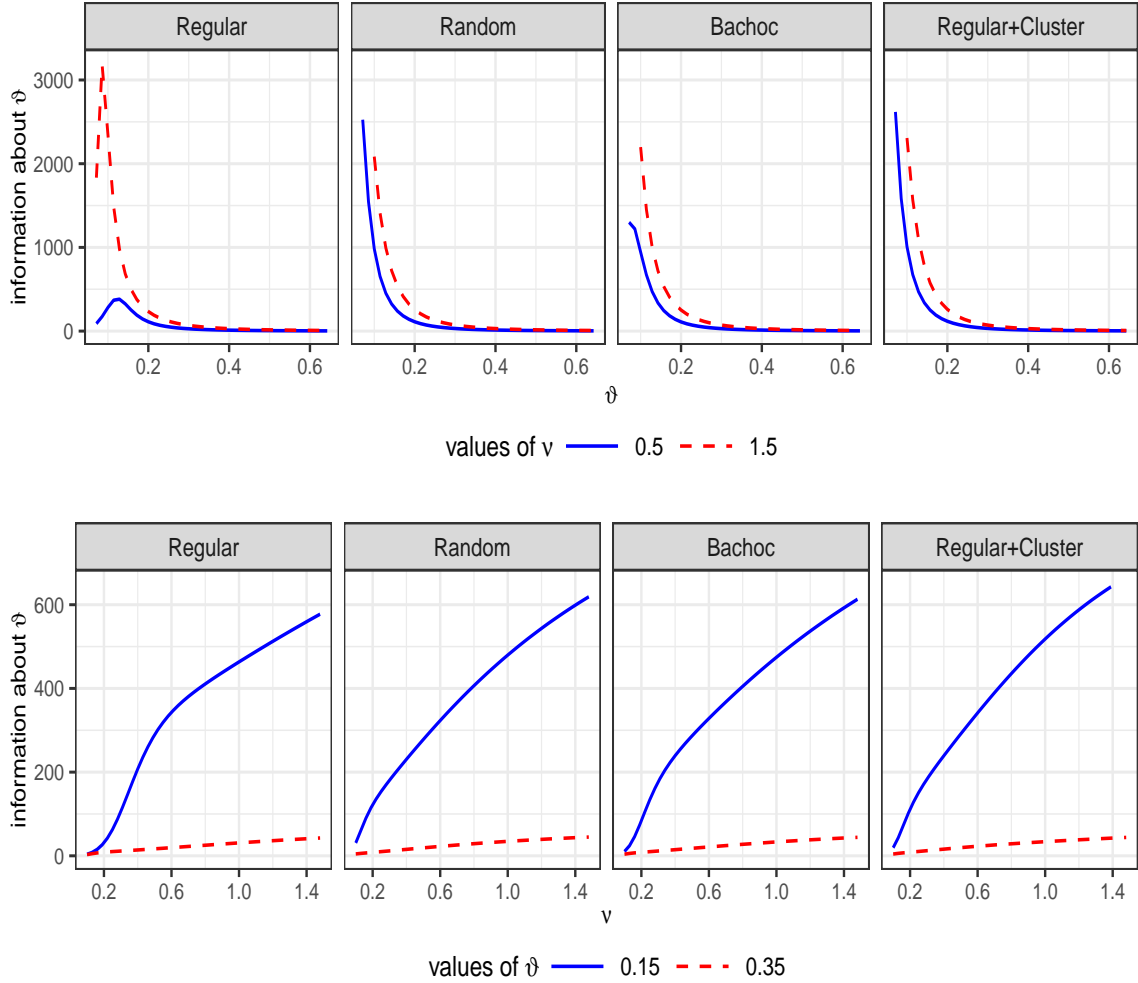
Figure 4: Plots of the information about the range parameter ϑ, $\mathrm{Inf}(\boldsymbol{\eta}, \mathcal{S}_n)_3$, for different sampling designs, $\sigma^2 = 1$ and $\tau^2 = 0.2$. Top: Information about ϑ as a function of ϑ for two values of ν. Bottom: Information about ϑ as a function of ν for two values of ϑ.

Figures 4 and 5 display the patterns of variation of the information about ϑ and ν, as functions of ϑ or ν, when $\sigma^2 = 1$ and $\tau^2 = 0.2$ are kept fixed. Extensive numerical explorations (not shown) reveal that the same general patterns hold for other values of σ^2 and τ^2. Also, the same patterns of variation were observed for other sample sizes ($n = 100$ and 529, not shown). In addition, it was seen that the same patterns of variation displayed in Figures 4 and 5 hold when ϑ and ν are fixed at other pairs of values; see also Figure 6 below. These numerical explorations also suggest that, when everything else (model and design) is kept fixed, the information about ϑ is generally an increasing function of σ^2 and a decreasing function of τ^2. The information about ν also appears to increase with σ^2 and decrease with τ^2, when everything else is kept fixed.

Information About the Range Parameter Relative to that of the Smoothness
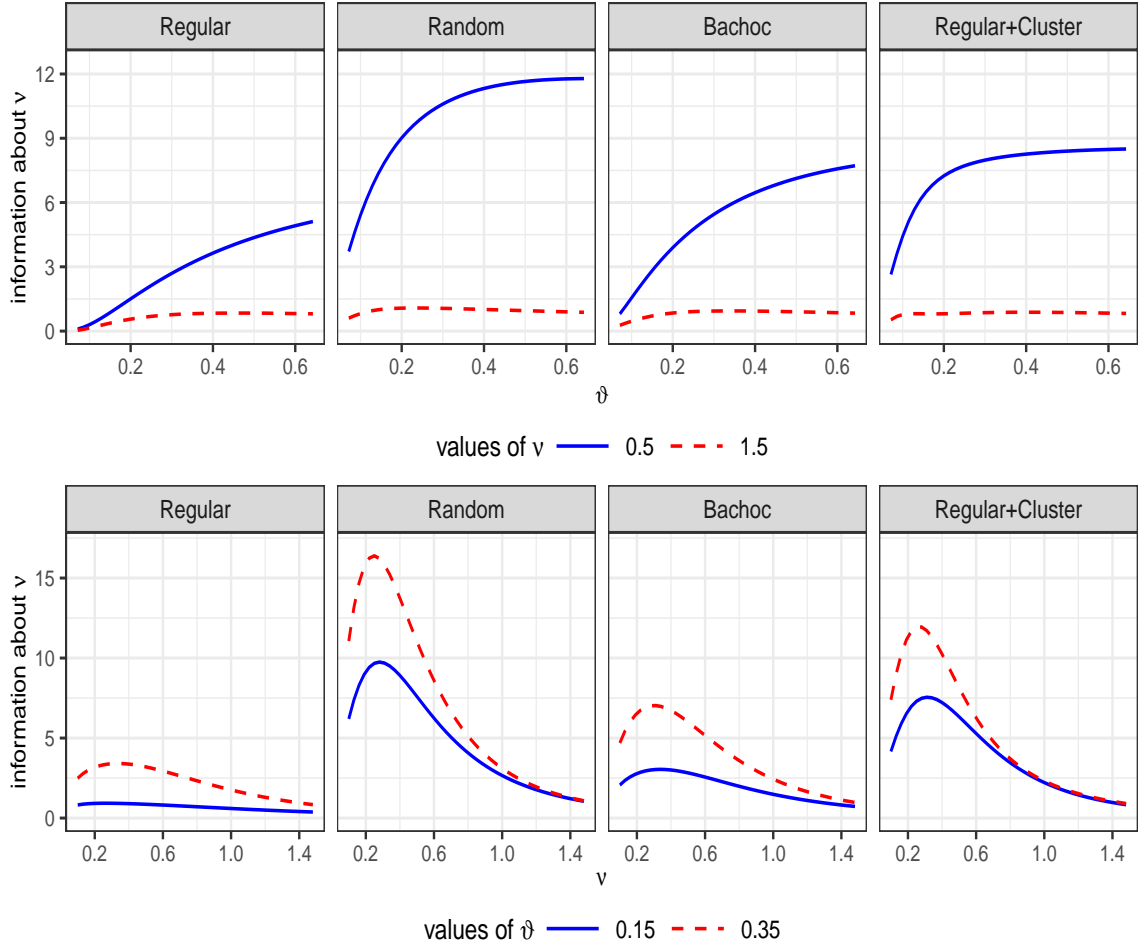
Figure 5: Plots of the information about the smoothness parameter ν, $\mathrm{Inf}(\boldsymbol{\eta}, \mathcal{S}_n)_4$, for different sampling designs, $\sigma^2 = 1$ and $\tau^2 = 0.2$. Top: information about ν as a function of ϑ for two values of ν. Bottom: information about ν as a function of ν for two values of ϑ.

Parameter. Now we investigate the variation of the information about the range parameter relative to the information about the smoothness parameter when (ϑ, ν) varies over the region $[0.05, 0.65] \times [0.1, 1.5]$. Figure 6 (top left) displays the contour plot of the ratio $\mathrm{Inf}(\boldsymbol{\eta}, \mathcal{S}_n)_3 / \mathrm{Inf}(\boldsymbol{\eta}, \mathcal{S}_n)_4$ when $\mathcal{S}_n$ is the regular design. It shows that this ratio is less than 1 in a region of the correlation parameter space that combines a large range parameter (strongly dependent process) and a small smoothness parameter (non–smooth process); it can be loosely described as the 'south–east' section of $[0.05, 0.65] \times [0.1, 1.5]$ and is denoted by T_{regular}. For these covariance models, the data contain substantial information about the smoothness parameter (when the information about the range parameter is used as reference). On the other hand, the opposite holds in T^c_{regular}, so for covariance models in this region the information about the smoothness parameter is less substantial. The same overall behavior occurs for the Random, Bachoc and Regular+Cluster designs, as shown
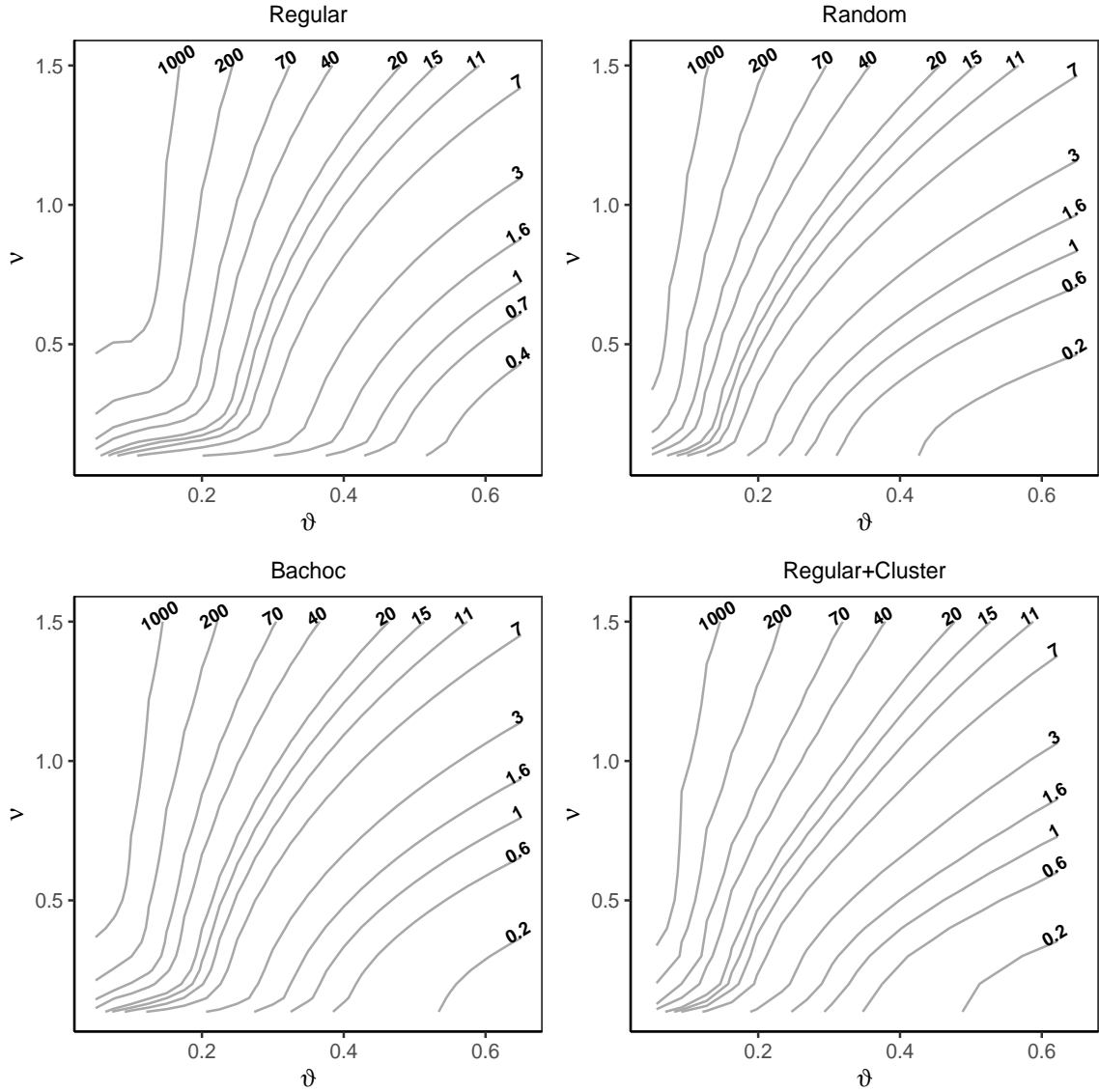
Figure 6: Contour plots of the ratio $\mathrm{Inf}(\boldsymbol{\eta}, \mathcal{S}_n)_3 / \mathrm{Inf}(\boldsymbol{\eta}, \mathcal{S}_n)_4$ for $\sigma^2 = 1$, $\tau^2 = 0.2$, (ϑ, ν) in a grid of points in $[0.1, 0.9] \times [0.1, 1.5]$ and different sampling designs.

in Figure 6, with the ratio $\mathrm{Inf}(\boldsymbol{\eta}, \mathcal{S}_n)_3 / \mathrm{Inf}(\boldsymbol{\eta}, \mathcal{S}_n)_4$ taking for each model values slightly smaller than those in the Regular design. In addition, if T_{random}, T_{bachoc} and $T_{\mathrm{reg+clu}}$ are defined similarly as T_{regular}, it generally holds that $T_{\mathrm{regular}} \subset T_{\mathrm{random}}$, $T_{\mathrm{regular}} \subset T_{\mathrm{bachoc}}$ and $T_{\mathrm{regular}} \subset T_{\mathrm{reg+clu}}$. Hence, for all the designs, the amount of information about the smoothness parameter is substantial when the true process is strongly dependent and non–smooth. Once again, the same behaviors were observed when σ^2 and τ^2 were fixed at other values.

Information About Another Microergodic Parameter. As indicated by a referee, a parameter that may be considered as relevant as ν for spatial interpolation/prediction

is $\zeta := \sigma^2/\vartheta^{2\nu}$, since it is also microergodic (Zhang, 2004). So we also investigate the pattern of variation of its information, both as a function of ϑ and as a function of ν. As for the other parameters, the information about ζ $(= \zeta(\boldsymbol{\eta}))$ is measured by the inverse of the Cramer–Rao lower bound for the variance of its unbiased estimators, which is given by (Keener, 2010, page 76)

$$i(\boldsymbol{\eta}, \mathcal{S}_n) := \left(\left(\nabla\zeta(\boldsymbol{\eta})\right)^\top I(\boldsymbol{\eta}, \mathcal{S}_n)^{-1}\nabla\zeta(\boldsymbol{\eta})\right)^{-1},$$

where

$$\nabla\zeta(\boldsymbol{\eta}) = \frac{1}{\vartheta^{2\nu}}\left(1, 0, -\frac{2\sigma^2\nu}{\vartheta}, -2\sigma^2\log(\vartheta)\right)^\top.$$

Figure 7 (top panels) displays plots of $i(\boldsymbol{\eta}, \mathcal{S}_n)$ as a function of ϑ when $\nu = 0.5$ and 1.5 for the four sampling designs. For both values of the smoothness parameter and all the designs the information about ζ increases monotonically when ϑ increases. Also, regardless of the design and the range parameter, the information about ζ is larger when $\nu = 0.5$ than when $\nu = 1.5$. This information is not very sensitive to the design, although it is a bit larger for the Random and Random+Cluster designs.

Figure 7 (bottom panels) displays plots of $i(\boldsymbol{\eta}, \mathcal{S}_n)$ as a function of ν when $\vartheta = 0.15$ and 0.35 for the four sampling designs. For both values of the range parameter and all the designs, the information about ζ increases up to a point and then decreases monotonically when ν increases. In addition, regardless of the design and the smoothness parameter, the information about ζ is larger when $\vartheta = 0.35$ than when $\vartheta = 0.15$. Finally, the comparison of Figure 7 with Figure 5 shows that the information about ν is larger than the information about ζ for all models and designs.

Variation of Information With Sample Size. Figure 8 displays the variation of the information about ϑ, ν and ζ with sample size for Random designs of size $n \leq 10000$ and the four models: (a) $\boldsymbol{\eta} = (1, 0.2, 0.2, 0.5)$, (b) $\boldsymbol{\eta} = (1, 0.2, 0.2, 1.5)$, (c) $\boldsymbol{\eta} = (1, 0.2, 0.4, 0.5)$ and (d) $\boldsymbol{\eta} = (1, 0.2, 0.4, 1.5)$. As expected, the information always increases with sample size, but the rate of change varies substantially depending on the model. For instance, for models (a) and (c) [non–smooth models] the rate of change of the information about ν is larger than that of the information about ϑ, while the opposite holds for models (b) and (d) [smooth models], at least when $n \leq 10000$. These plots again show that for some models and sample sizes the information about ν is larger than that about ϑ. The information about ζ and its rate of change appear small for all models, showing again that this information is smaller than the information about ν. The aforementioned behaviors were found to also hold for Regular designs of size $n \leq 10000$ (not shown).
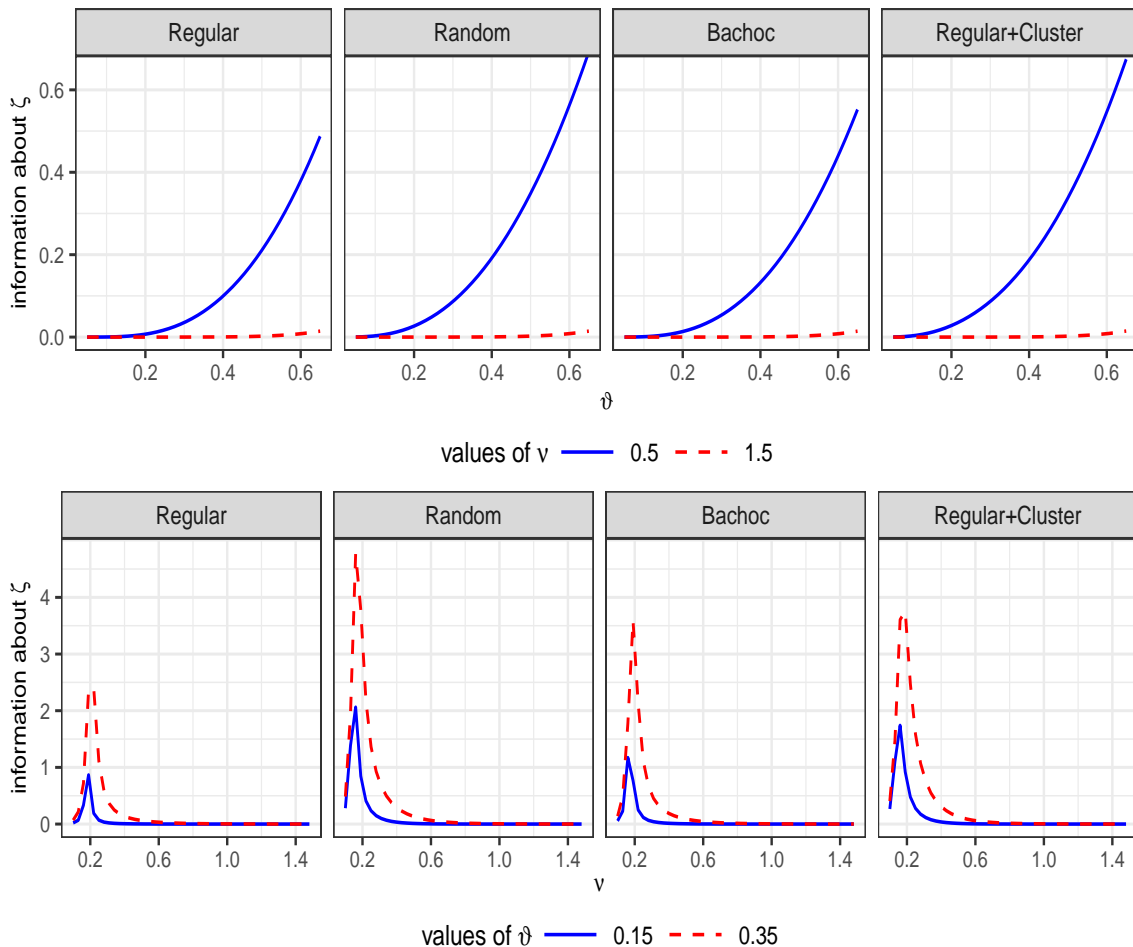
Figure 7: Plots of the information about the microergodic parameter ζ, $i(\boldsymbol{\eta}, \mathcal{S}_n)$, for different sampling designs, $\sigma^2 = 1$ and $\tau^2 = 0.2$. Top: information about ζ as a function of ϑ for two values of ν. Bottom: information about ζ as a function of ν for two values of ϑ.

5 Local Model Influence

An indirect but related approach to assess the information the data have about the covariance parameters is to quantify how sensitive the likelihood function is to small changes of the covariance parameters. Assume $p = 1$ and $\beta = 0$, so $\boldsymbol{\eta}$ are the only model parameters. McCulloch (1989) suggested a way to do this by carrying out an eigen–analysis of the (estimated) Fisher information matrix, which is related to the Kullback–Leibler divergence of the true model from the estimated model. Specifically, let $(\lambda^*, \boldsymbol{\delta}^*)$ be an eigenpair of $I(\hat{\boldsymbol{\eta}}, \mathcal{S}_n)$, where λ^* is its largest eigenvalue and $\boldsymbol{\delta}^*$ is the corresponding eigenvector of unit Euclidean length. Then, values of λ^* larger than 1 indicate that the likelihood function is sensitive to small changes of the covariance parameters, while the opposite holds when λ^* is close to 0. Additionally, the components of $\boldsymbol{\delta}^*$ indicate the coefficients of the linear
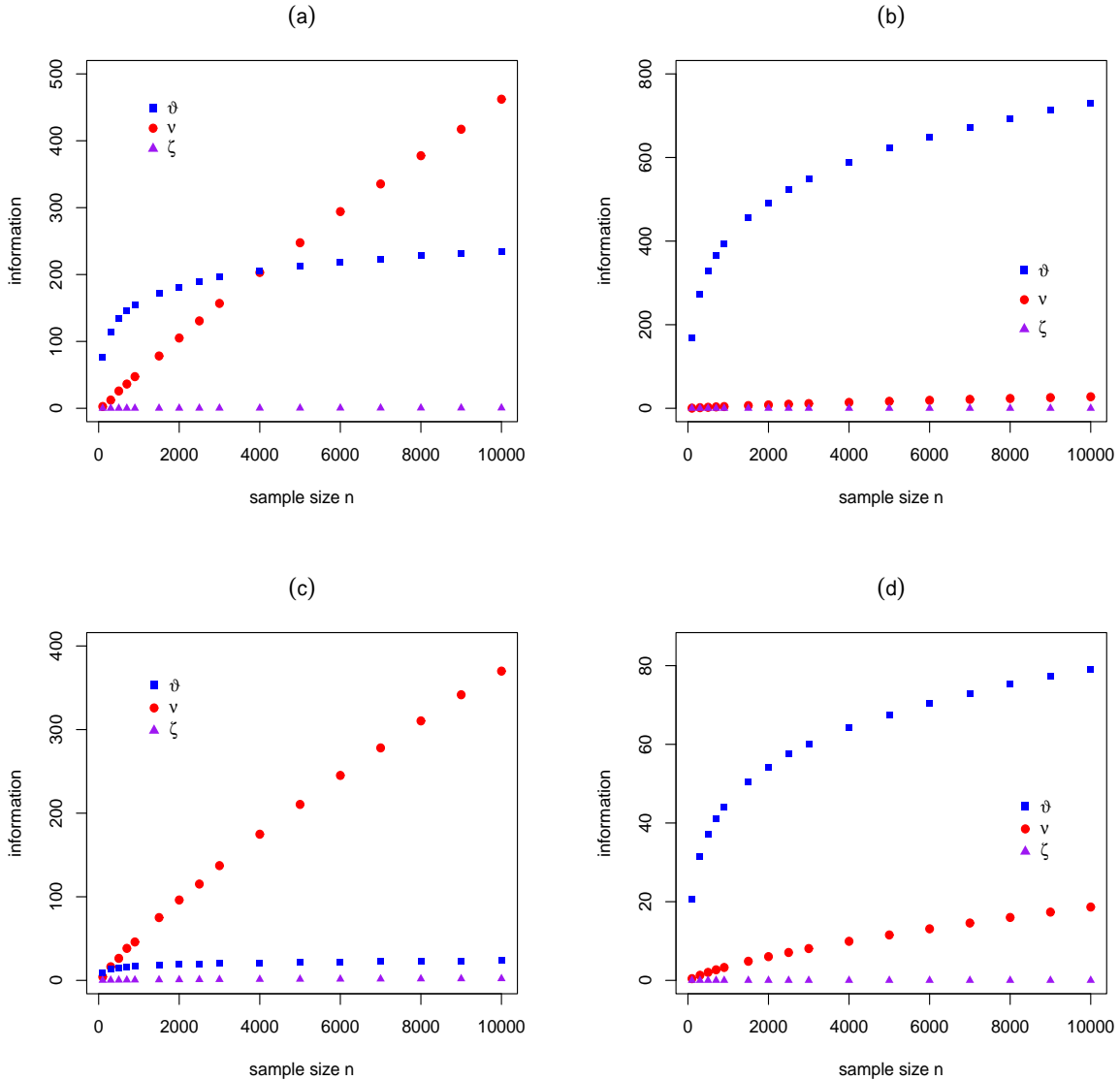
Figure 8: Plots of the information about ϑ, ν and ζ versus sample size for the Random sampling design of size n and the models: (a) $\boldsymbol{\eta} = (1, 0.2, 0.2, 0.5)$, (b) $\boldsymbol{\eta} = (1, 0.2, 0.2, 1.5)$, (c) $\boldsymbol{\eta} = (1, 0.2, 0.4, 0.5)$ and (d) $\boldsymbol{\eta} = (1, 0.2, 0.4, 1.5)$.

combination of $\boldsymbol{\eta}$ that is most influential. See McCulloch (1989) for details, and how to use this idea to assess the effects of small changes of a prior distribution on the corresponding posterior and predictive distributions.

5.1 A Telling Example (Continuation)

We now revise and extend the analysis of the Swiss rainfall data in Section 3.2 using the exact Fisher information matrix computed as described in Section 4.2, and re–scaling the spatial coordinates as described in Section 4.3, with $r_{\max} = 335.71$ kilometers. The inverse of the

Fisher information matrix evaluated at the MLE $\hat{\boldsymbol{\eta}} = (\hat{\sigma}^2, \hat{\tau}^2, \hat{\vartheta}, \hat{\nu}) = (105.40, 6.72, 0.22, 0.96)$ is

$$
I(\hat{\boldsymbol{\eta}}, \mathcal{S}_n)^{-1} = \begin{pmatrix} 1486.721 & -5.233 & 2.156 & -2.313 \\ -5.233 & 1.273 & -0.031 & 0.209 \\ 2.156 & -0.031 & 0.005 & -0.013 \\ -2.313 & 0.209 & -0.013 & 0.064 \end{pmatrix}.
$$

The (estimated) information about the covariance parameters is

$$
\mathrm{Inf}(\hat{\boldsymbol{\eta}}, \mathcal{S}_n) = (0.001, 0.786, 199.297, 15.643),
$$

confirming again that these data have substantial information about the smoothness parameter. The effect of re–scaling the spatial coordinates on the Fisher information matrix is to produce large changes in the third row and third column while leaving the remaining entries almost unchanged (when compared to not re–scaling). This largely changes the information about the range parameter while leaving the information about the other covariance parameters almost unaffected.

We also investigate the local influence of small changes of the covariance parameters on the likelihood. For the Swiss rainfall data the largest eigenvalue of $I(\hat{\boldsymbol{\eta}}, \mathcal{S}_n)$ and its corresponding eigenvector are, respectively,

$$
\lambda^* = 3.37 \times 10^3 \quad \text{and} \quad \boldsymbol{\delta}^* = (-0.001, -0.014, 0.980, 0.200)^\top.
$$

This indicates that, for these data, the likelihood is sensitive to small changes of the covariance parameters, since $\lambda^* \gg 1$, and the range and smoothness parameters are the most influential, since their corresponding coefficients in $\boldsymbol{\delta}^*$ have the largest magnitudes.

6   Conclusions and Discussion

This work explored the patterns of variation of the information about the correlation parameters of the Matérn model in Gaussian random fields. Using the inverse diagonal elements of the inverse of the Fisher information matrix as an information measure, it was shown that the information about these correlation parameters varies substantially depending on the true model and sampling design. Specifically, the following conclusions follow from the numerical explorations in Section 4.3:

1. In general, the information about the range parameter ϑ displays little sensitivity to the sampling design.

2. Except for weakly correlated processes observed on a regular design, the information about ϑ decreases when ϑ increases, to the point of being very small for processes with strong correlation.

3. The information about ϑ increases when ν increases. This information is largest for processes with weak correlation that are smooth.

4. The information about the smoothness parameter ν does display sensitivity to the sampling design. The Regular design is the least informative about ν, while the Random design is the most informative.

5. The information about ν increases when ϑ increases. This information is the largest for processes with strong correlation that are non–smooth.

6. The information about ν does not display a monotonic pattern of change with ν.

7. Overall and regardless of the design, the information about the smoothness parameter ν is substantial for processes with strong correlation that are non–smooth.

8. The information about the microergodic parameter ζ increases when ϑ increases and does not changes monotonically when ν increases. In general this information is smaller than the information about ν.

9. The information about ϑ, ν and ζ grows with sample size, but the rate of change varies substantially with the true model. The rate of change of information about ν is fastest for non–smooth processes, while the rate of change of information about ζ appear always small.

Some of the above conclusions confirm similar empirical findings reported in the literature, while other conclusions cast doubts on the unqualified claim regarding geostatistical data having little or no information about the smoothness parameter of the Matérn model, as well as the common practice of fixing this parameter at some customary value (e.g., $\nu = 0.5$ or 1.5). The analysis of the Swiss rainfall data provided an example where the data contain substantial information about the smoothness parameter. These findings call for a reassessment of this practice and a shift toward a more statistically sound practice where inferences about the random field rely on data–based estimates of both correlation parameters, at least for strongly dependent and non–smooth processes observed on irregular sampling designs. For instance, McCullagh and Clifford (2006) provided evidence showing that data from crop yield processes tend to possess these features.

Although the above findings were obtained for Gaussian random fields, they also hold for some non–Gaussian random fields. For instance, this is the case for some transformed Gaussian random fields (e.g., log–Gaussian random fields) since the Fisher information matrix is invariant under differentiable one–to–one transformations of the data. Also, although the study was restricted to the Matérn family of covariance functions, we conjecture that the above findings also hold for other families of covariance functions, such as the generalized

Wendland (Bevilacqua et al., 2019) and power exponential (De Oliveira, Kedem, and Short, 1997) families that, as the Matérn, depend on a smoothness or roughness parameter.

The approach presented in Section 4.2 to compute $(\partial/\partial\nu)K_{\vartheta}(r)$ might not be fast or accurate enough to compute the expected or observed Fisher information matrices used in iterative algorithms for the computation of maximum likelihood estimates based on large data sets. Recently, Geoga, Marin, Schanen, and Stein (2022) developed methods and software for fast and accurate computation of this derivative using automatic differentiation based on a new implementation of the Bessel function $\mathcal{K}_{\nu}(x)$. These should contribute to ameliorate the computational challenges of estimating all the parameters in the Matérn family.

Acknowledgment

Appendix

Derivation of Identities (4.6) and (4.7)

To derive (4.6), write the Matérn correlation function as $K_{\vartheta}(r) = c(\nu)b(\vartheta)^{\nu}\mathcal{K}_{\nu}(b(\vartheta))$, where $c(\nu) := 2^{1-\nu}/\Gamma(\nu)$ and $b(\vartheta) := 2r\sqrt{\nu}/\vartheta$. Then by direct differentiation

$$
\begin{aligned}
\frac{\partial}{\partial\vartheta}K_{\vartheta}(r) &= c(\nu)\Big(\nu b(\vartheta)^{\nu-1}b'(\vartheta)\mathcal{K}_{\nu}(b(\vartheta)) + b(\vartheta)^{\nu}\frac{\partial}{\partial x}\mathcal{K}_{\nu}(x)\Big|_{x=b(\vartheta)}\cdot b'(\vartheta)\Big) \\
&= c(\nu)b(\vartheta)^{\nu-1}b'(\vartheta)\Big(\nu\mathcal{K}_{\nu}(b(\vartheta)) - b(\vartheta)\Big[\mathcal{K}_{\nu-1}(b(\vartheta)) + \frac{\nu\vartheta}{2\sqrt{\nu}r}\mathcal{K}_{\nu}(b(\vartheta))\Big]\Big) \\
&= -\frac{c(\nu)(2\sqrt{\nu}r)^{\nu}}{\vartheta^{\nu+1}}\Big(\nu\mathcal{K}_{\nu}\Big(\frac{2\sqrt{\nu}}{\vartheta}r\Big) - \frac{2\sqrt{\nu}}{\vartheta}r\mathcal{K}_{\nu-1}\Big(\frac{2\sqrt{\nu}}{\vartheta}r\Big) - \nu\mathcal{K}_{\nu}\Big(\frac{2\sqrt{\nu}}{\vartheta}r\Big)\Big) \\
&= \frac{4\nu^{\frac{\nu+1}{2}}r^{\nu+1}}{\Gamma(\nu)\vartheta^{\nu+2}}\mathcal{K}_{\nu-1}\Big(\frac{2\sqrt{\nu}}{\vartheta}r\Big),
\end{aligned}
$$

where the second identity follows from (4.3).

To derive (4.7), write the Matérn correlation function as

$$
K_{\vartheta}(r) = 2e^{\nu\log(1/2)}(\Gamma(\nu))^{-1}e^{\nu\log(\frac{2r}{\vartheta}\sqrt{\nu})}\mathcal{K}_{\nu}\Big(\frac{2r}{\vartheta}\sqrt{\nu}\Big),
$$

so after direct differentiation we have

$$\frac{\partial}{\partial \nu}K_{\boldsymbol{\vartheta}}(r) = \left(\frac{1}{2} + \log\left(\frac{\sqrt{\nu}}{\vartheta}r\right) - \psi(\nu)\right)K_{\boldsymbol{\vartheta}}(r) + h(\nu)\frac{\partial}{\partial \nu}\mathcal{K}_{\nu}\left(\frac{2r}{\vartheta}\sqrt{\nu}\right). \qquad (6.1)$$

Now, let $G(x,y) := \mathcal{K}_x(y)$. Then

$$\begin{aligned}
\frac{\partial}{\partial \nu}\mathcal{K}_{\nu}\left(\frac{2r}{\vartheta}\sqrt{\nu}\right) &= \frac{\partial}{\partial \nu}G\left(\nu, \frac{2r}{\vartheta}\sqrt{\nu}\right) \\
&= \frac{\partial}{\partial x}G(x,y)\Big|_{x=\nu, y=\frac{2r}{\vartheta}\sqrt{\nu}} + \frac{\partial}{\partial y}G(x,y)\Big|_{x=\nu, y=\frac{2r}{\vartheta}\sqrt{\nu}}\cdot\frac{r}{\vartheta\sqrt{\nu}} \\
&= \int_0^\infty t\sinh(\nu t)e^{-\frac{2r}{\vartheta}\sqrt{\nu}\cosh(t)}dt \\
&\quad - \frac{r}{\vartheta\sqrt{\nu}}\left(\mathcal{K}_{\nu-1}\left(\frac{2r}{\vartheta}\sqrt{\nu}\right) + \frac{\vartheta\sqrt{\nu}}{2r}\mathcal{K}_{\nu}\left(\frac{2r}{\vartheta}\sqrt{\nu}\right)\right) \\
&= \int_0^\infty t\sinh(\nu t)e^{-\frac{2r}{\vartheta}\sqrt{\nu}\cosh(t)}dt - \frac{r}{\vartheta\sqrt{\nu}}\mathcal{K}_{\nu-1}\left(\frac{2r}{\vartheta}\sqrt{\nu}\right) - \frac{1}{2}\mathcal{K}_{\nu}\left(\frac{2r}{\vartheta}\sqrt{\nu}\right),
\end{aligned}$$
$$(6.2)$$

where the third identity follows from (4.3) and (4.5). Finally, replacing (6.2) into (6.1) we get

$$\begin{aligned}
\frac{\partial}{\partial \nu}K_{\boldsymbol{\vartheta}}(r) &= \frac{1}{2}K_{\boldsymbol{\vartheta}}(r) + \left(\log\left(\frac{\sqrt{\nu}}{\vartheta}r\right) - \psi(\nu)\right)K_{\boldsymbol{\vartheta}}(r) + h(\nu)\int_0^\infty t\sinh(\nu t)e^{-\frac{2r}{\vartheta}\sqrt{\nu}\cosh(t)}dt \\
&\quad - h(\nu)\frac{r}{\vartheta\sqrt{\nu}}\mathcal{K}_{\nu-1}\left(\frac{2r}{\vartheta}\sqrt{\nu}\right) - \frac{1}{2}\underbrace{h(\nu)\mathcal{K}_{\nu}\left(\frac{2r}{\vartheta}\sqrt{\nu}\right)}_{K_{\boldsymbol{\vartheta}}(r)} \\
&= \left(\log\left(\frac{\sqrt{\nu}}{\vartheta}r\right) - \psi(\nu)\right)K_{\boldsymbol{\vartheta}}(r) \\
&\quad - h(\nu)\left(\frac{r}{\vartheta\sqrt{\nu}}\mathcal{K}_{\nu-1}\left(\frac{2r}{\vartheta}\sqrt{\nu}\right) - \int_0^\infty t\sinh(\nu t)e^{-\frac{2r}{\vartheta}\sqrt{\nu}\cosh(t)}dt\right).
\end{aligned}$$

References

Bachoc, F. (2014). Asymptotic analysis of the role of spatial sampling for covariance parameter estimation of Gaussian processes. *Journal of Multivariate Analysis 125*, 1–35.

Bevilacqua, M., T. Faouzi, R. Furrer, and E. Porcu (2019). Estimation and prediction using generalized Wendland covariance functions under fixed domain asymptotics. *The Annals of Statistics 47*, 828–856.

Bose, M., J. Hodges, and S. Banerjee (2018). Toward a diagnostic toolkit for linear models with Gaussian–process distributed random effects. *Biometrics 74*, 863–873.

Cressie, N. (1993). *Statistics for Spatial Data (rev. ed.)*. Wiley.

De Oliveira, V., B. Kedem, and D. Short (1997). Bayesian prediction of transformed Gaussian random fields. *Journal of the American Statistical Association 92*, 1422–1433.

Diggle, P. and S. Lophaven (2006). Bayesian geostatistical design. *Scandinavian Journal of Statistics 33*, 53–64.

Diggle, P. and P. Ribeiro (2007). *Model–Based Geostatistics*. Springer–Verlag.

Gelfand, A. and E. Schliep (2016). Spatial statistics and Gaussian processes: A beautiful marriage. *Spatial Statistics 18*, 86–104.

Geoga, C., O. Marin, M. Schanen, and M. Stein (2022). Fitting Matérn smoothness parameters using automatic differentiation. *arXiv:2201.00090v1*.

Gradshteyn, T. and I. Ryzhik (2000). *Table of Integrals, Series, and Products, 6th edition*. Academic Press.

Guttorp, P. and T. Gneiting (2006). Studies in the history of probability and statistics XLIX on the Matérn correlation family. *Biometrika 93*, 989–995.

Handcock, M. and M. Stein (1993). A Bayesian analysis of kriging. *Technometrics 35*, 403–410.

Kaufman, C. and B. Shaby (2013). The role of the range parameter for estimation and prediction in geostatistics. *Biometrika 100*, 473–484.

Keener, R. (2010). *Theoretical Statistics: Topics for a Core Course*. Springer.

Loh, W.-L. (2015). Estimating the smoothness of a Gaussian random field from irregularly spaced data via higher–order quadratic variations. *The Annals of Statistics 43*, 2766–2794.

Loh, W.-L., S. Sun, and J. Wen (2021). On fixed–domain asymptotics, parameter estimation and isotropic Gaussian random fields with Matérn covariance functions. *The Annals of Statistics 49*, 3127–3152.

Matérn, B. (1986). *Spatial Variation* (2nd ed.). Springer–Verlag.

McCullagh, P. and D. Clifford (2006). Evidence for conformal invariance of crop yields. *Proceedigns of the Royal Society A 462*, 2119–2143.

McCulloch, R. (1989). Local model influence. *Journal of the American Statistical Association 84*, 473–478.

Papritz, A. and C. Schwierz (2021). `georob`: Robust geostatistical analysis of spatial data. *R package version 0.3-14*.

Seber, G. and C. Wild (2003). *Nonlinear Regression*. Wiley.

Stein, M. (1988). Asymptotically efficient prediction of a random field with a misspecified covariance function. *The Annals of Statistics 16*, 55–63.

Stein, M. (1990). Uniform asymptotic optimality of linear predictions of a random field using an incorrect second–order structure. *The Annals of Statistics 18*, 850–872.

Stein, M. (1993). A simple condition for asymptotic optimality of linear predictions of random fields. *Statistics & Probability Letters 17*, 399–404.

Stein, M. (1999). *Interpolation of Spatial Data: Some Theory for Kriging*. Springer–Verlag.

Steiner, M., R. Houze, and S. Yuter (1995). Climatological characterization of three–dimensional structure from operational radar and gauge data. *Journal of Applied Meteorology 34*, 1978–2007.

Wu, W.-Y. and C. Lim (2016). Estimation of smoothness of a stationary Gaussian random field. *Statistica Sinica 26*, 1729–1745.

Wu, W.-Y., C. Lim, and Y. Xiao (2013). Tail estimation of the spectral density for a stationary Gaussian random field. *Journal of Multivariate Analysis 116*, 74–91.

Zhang, H. (2004). Inconsistent estimation and asymptotically equal interpolations in model–based geostatistics. *Journal of the American Statistical Association 99*, 250–261.

Zhu, Z. and M. Stein (2005). Spatial sampling design for parameter estimation of the covariance function. *Journal of Statistical Planning and Inference 134*, 583–603.

Zhu, Z. and M. Stein (2006). Spatial sampling design for prediction with estimated parameters. *Journal of Agricultural, Biological, and Environmental Statistics 11*, 24–44.

Zhu, Z. and H. Zhang (2006). Spatial sampling design under the infill asymptotic framework. *Environmetrics 17*, 323–337.

Zimmerman, D. (2006). Optimal network design for spatial prediction, covariance parameter estimation, and empirical prediction. *Environmetrics 17*, 635–652.

Zimmerman, D. (2010). *Likelihood–Based Methods. In: Handbook of Spatial Statistics, A.E. Gelfand, P.J. Diggle, M. Fuentes and P. Guttorp (eds.)*. CRC Press, 45-56.